UNCERTAINTY OF THE NIST LOW FROST-POINT HUMIDITY GENERATOR

G. E. Scace, J. T. Hodges

National Institute of Standards and Technology, Gaithersburg, Maryland, USA

ABSTRACT

The NIST Low Frost-point Humidity Generator (LFPG) produces water vapor – gas mixtures with mole fractions from approximately 5 nmol/mol to 4 mmol/mol for research, calibration of transfer standards, and testing and development of new humidity instrumentation. The LFPG generates these mixtures by saturating air or nitrogen with water vapor over a plane surface of ice maintained under conditions of constant temperature and pressure. Uncertainties in pressure and temperature determine the ultimate accuracy limit of the LFPG when humidity is expressed as frost-point temperature. Uncertainties in the correlations predicting vapor pressure and non-ideal gas effects (enhancement factor) dominate when knowledge of mole fraction is required. This paper describes the LFPG in sufficient detail to frame a discussion of inherent uncertainties. Uncertainties in the various subsystems are discussed and the expanded uncertainties in water vapor mole fraction and frost-point temperature are presented.

1. INTRODUCTION

As new microelectronics manufacturing technologies have emerged, increased emphasis has been placed on the accurate measurement of water vapor mole fractions below 1 μmol/mol. Strict monitoring and control of trace (10 nmol/mol and lower) levels of water vapor are required in micro-electronics fabrication processes. Regrettably, metrology-grade standards have not been available to verify and characterize the performance of existing hygrometers and existing humidity instrumentation. To address these technical issues, NIST has developed a thermodynamically based humidity generator, referred to as the low frost-point generator (LFPG). Its output spans six decades, covering the range 5 nmol/mol to 4 mmol/mol, in mole fraction of water vapor. In this paper, we present and discuss the uncertainty of the LFPG.

2. PRINCIPLE OF OPERATION AND DESCRIPTION OF APPARATUS

The LFPG saturates an inert gas stream with water vapor by flowing the gas over a plane surface of isothermal ice at known temperature and pressure. By ensuring that the inlet gas stream has reached thermodynamic equilibrium with the generator saturator, the mole fraction, *x*, of water vapor in the gas phase can be calculated from known thermodynamic properties, and is proportional to the vapor pressure of the ice $e_w(T)$ and the enhancement factor $f(T,P)$. This latter quantity is close to unity and accounts for departures from ideal solution behavior as well as non-ideal gas effects [1-3]. Assuming that the saturator ice and sample stream are in local thermodynamic equilibrium, then, at a total pressure P_s and system absolute temperature T_s, the mole fraction of water vapor is

$$x = \frac{e_w(T_s)}{P_s} f(T_s, P_s), \tag{1}$$

in which the subscript *s* indicates conditions in the saturator. Equation 1 is the central theoretical basis for the use of the low frost-point generator as a humidity standard.

Measurements of the gas frost-point temperature T_h made downstream of the saturator (as for example with a chilled mirror hygrometer) must be related to the saturator conditions. Assuming that x is conserved, and assuming that the sensor and sample stream are in local thermodynamic equilibrium, then

$$x = \frac{e_w(T_s)}{P_s} f(T_s, P_s) = \frac{e_w(T_h)}{P_h} f(T_h, P_h) \quad , \tag{2}$$

in which the subscript h, indicates conditions in the hygrometer.

The LFPG embodies the simplest form of saturator-based humidity generator and is described in detail in [4]. The LFPG's cylindrical copper saturator contains a 4.9-m long ice-coated passageway. The saturator, which is 195 mm in diameter and 125 mm in height, resides in a vacuum chamber for thermal isolation. Two thermoelectric heat pump arrays and a mechanical refrigeration system control the saturator temperature to within 2 mK, and an electronic back-pressure regulator controls the saturator pressure to within 10 Pa. The operating temperature and pressure ranges are –10 EC to –100 EC, and 100 kPa to 300 kPa, respectively. The saturated gas is piped to various hygrometers *via* heated electropolished stainless steel tubing. A fraction of the gas flows through the hygrometer, while the remainder exhausts to the room. For volumetric flow rates up to 5 L/min, the pressure drop through the tubing connecting the saturator to hygrometers is typically less than 200 Pa.

The combined expanded uncertainties of x and T_h were calculated according to ISO practice using Eq. 2 as the basis for combining the uncertainty components [5]. These uncertainty components are discussed below. All expanded uncertainties reported in this paper are based on a coverage factor k=2.

3. PRESSURE UNCERTAINTY

A quartz bourdon tube and a piezo-resistive gauge measure the pressures within the saturator and atmosphere, respectively. Atmospheric pressure is monitored only when the humidity unit of interest is frost-point temperature and the hygrometer is designed to operate near ambient pressure. Saturator pressure is always measured. When constant water vapor mole fractions are desired, the saturator pressure measurement data are also used for feedback control of the back-pressure regulator. The measurement uncertainty analysis for both gauges considers uncertainty in gauge calibration, calibration drift, gauge precision, and daily zero drift. Calibrations are performed using a piston gauge and stainless steel weights calibrated at NIST. Variations in the saturator pressure associated with the finite resolution of the pressure control system are added in quadrature to the measurement uncertainty to yield the combined standard uncertainty of P_s, summarized in Figure 1. The dominant uncertainty arises from calibration drift, which could be reduced by greater calibration frequency. The combined standard uncertainty of the piezo-resistive pressure gauge used to measure P_h is 16 Pa.

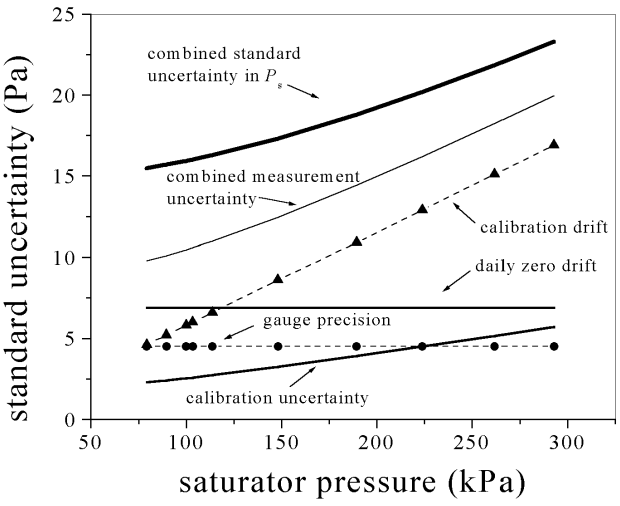

Figure 1: Sources of uncertainty in the determination of P_s.

4. TEMPERATURE UNCERTAINTY

A standard platinum resistance thermometer (SPRT) measures T_s, with the thermometer resistance related to temperature per ITS-90 [6]. The resistance of the SPRT is measured by sequentially flowing DC current from a stable current source through a Wilkins reference resistor and the SPRT. Voltage measurements across the thermometer and the resistor are made in both "forward" and "reverse" current directions. The magnitudes of the voltage readings are averaged to cancel out the electromotive force produced by temperature differences that are inherent to the measurement system's connections and wiring. Multiplying the voltage ratio by the value of the reference resistance yields the thermometer resistance.

Uncertainty of the SPRT resistance obtained by the DC voltage ratio technique depends on the short-term stability of the current source, standard resistor, and voltmeter. In addition, voltmeter linearity, zero drift, and reference resistor calibration uncertainty must be considered. Over short time intervals, the change in reference resistor values and voltmeter response is nil. Enabling the auto-zeroing feature on the voltmeter minimizes zero drift, leaving short-term current source stability, and reference resistor calibration uncertainty as the dominant contributors to resistance measurement uncertainty. Water triple point measurements are periodically made as part of the maintenance program of the LFPG. The SPRT resistance obtained in the water triple point cell is used to calculate the resistance ratio $W(\underline{T}_{90})$ as defined by ITS-90. Since the triple point measurements may have been made some months prior to the saturator temperature measurements of interest, long-term stability of the Wilkens resistor must also be considered in the uncertainty analysis. The maximum combined standard uncertainty of the temperature measurement, including the uncertainty propagated by the calibration uncertainties at each fixed point (argon, mercury, water triple points), is 0.0024 °C.

The temperature throughout the saturator deviates slightly from the measured temperature and adds an additional uncertainty to T_s. The most important mechanisms inducing temperature non-uniformity include sensible heat exchange between the incoming gas and the saturator and performance variations among the eight thermo-electric heat pumps. Measurements of saturator temperature non-uniformity were made throughout the saturator temperature range of the LFPG using a second NIST-calibrated SPRT and the measurement system described above. The standard uncertainty due to temperature non-uniformity is 0.0058 °C, which constitutes the largest component of uncertainty in

T_s. The combined standard uncertainty of T_s is 0.006 °C, and is obtained by adding in quadrature the uncertainties associated with temperature measurement and temperature non-uniformity.

5. VAPOR PRESSURE AND ENHANCEMENT FACTOR UNCERTAINTY

The uncertainty of the vapor pressure of ice $e_w(T)$ was calculated by combining the uncertainty published by Wexler [1] with the additional uncertainty in $e_w(T)$ contributed by the propagation of uncertainty in T_s. The uncertainty of the enhancement factor for water vapor / air mixtures, $f(T,P)$, was similarly calculated by combining the uncertainty published by Hyland and Wexler [2,3] with the additional uncertainties in $f(T,P)$ contributed by the propagation of temperature and pressure uncertainties. The relative expanded uncertainties of $e_w(T)$, and $f(T,P)$ are shown in Fig. 2.

Although vapor pressure and enhancement factor measurement data are sparse, use of uncertainty values published in the work of Hyland and Wexler is justified. Both Wexler's ice vapor pressure formulation and Hyland and Wexler's predictions of enhancement factor are based on thermodynamics, with the uncertainty values based on the uncertainties of the thermodynamic variables and constants used in their calculations. Measurements of $e_w(T)$ have yet to be made with sufficient precision to dispute Wexler's vapor pressure formulation.

Instrumentation used to measure water vapor mole fractions in the nmol/mol range is often incompatible with oxygen and commonly uses pure nitrogen rather than air as the carrier gas. For lack of better data, we use the enhancement factor values for air, recognizing that nitrogen is the primary constituent of air. We intend to calculate $f(T,P)$ for nitrogen in the future. As shown below, the effect of uncertainty in $f(T,P)$ on frost-point temperature is negligible for the small pressure differences P_s - P_h considered here. Consequently, the composition of the carrier gas has little effect on T_h.

6. LFPG OUTPUT UNCERTAINTY

The combined relative expanded uncertainty in x, and the respective contributions to this quantity that are associated with uncertainties in $e_w(T)$, $f(T,P)$ and P_s, are presented in Fig.2.

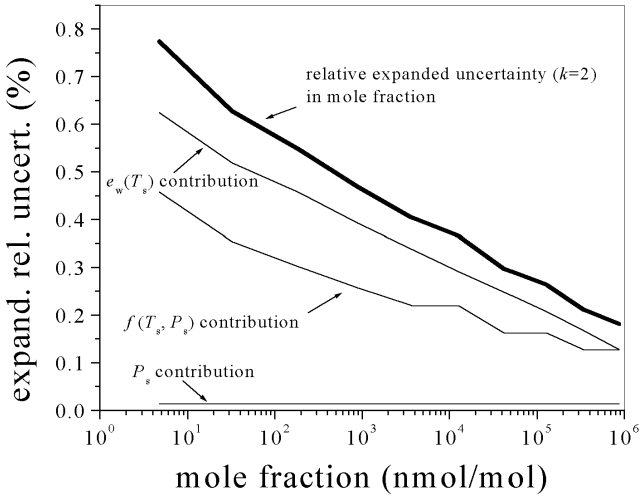

Figure 2: Expanded (k=2) relative uncertainty in water vapor mole fraction based on P_s = 300 kPa.

We evaluated the uncertainty in $f(T,P)$ at the maximum operating saturator pressure for the LFPG, given by $P_{s,max} \approx 300$ kPa. Since the uncertainty in the enhancement factor increases with pressure, this relatively high-pressure condition corresponds to the maximum uncertainty in $f(T,P)$. As illustrated in Fig. 2, the dominant contributions to the uncertainty in x are associated with $e_w(T)$ and $f(T,P)$, and uncertainty in the determination of P_s has a negligible effect on the combined uncertainty of x.

The frost-point temperature at the hygrometer is $T_h = T_s - \Delta T$, where ΔT is the reduction in condensation temperature caused by expansion of the gas mixture between the saturator and the hygrometer. Therefore, the uncertainty of T_h must consider the uncertainties in T_s and ΔT. To estimate ΔT and its uncertainty, we define Δe_w as the difference between $e_w(T_s)$, and the vapor pressure of ice evaluated at the hygrometer temperature $e_w(T_h)$. This quantity is expressed in terms of $e_w(T_s)$, the derivative of the natural logarithm of vapor pressure with respect to temperature η, and ΔT. For small values of ΔT (*i.e.*, . 20 mK) such as those associated with the 500 Pa maximum pressure drop $P_s - P_h$ considered in our analysis, η is constant to within 2 parts in 10^4. In this limit, we approximate Δe_w as,

$$\Delta e_w \cong \frac{de_w(T_s)}{dT}\Delta T = e_w(T_s)\frac{d\ln e_w(T_s)}{dT}\Delta T = e_w(T_s)\eta\Delta T \quad . \tag{3}$$

The preceding equation allows expression of $e_w(T_h)$ in terms of $e_w(T_s)$, η and ΔT as,

$$e_w(T_h) = e_w(T_s) - \Delta e_w = e_w(T_s)(1-\eta\Delta T). \tag{4}$$

Substituting into Eq.2 and solving for ΔT, gives

$$\Delta T = \left(1 - \frac{P_h}{P_s}\frac{f(T_s,P_s)}{f(T_h,P_h)}\right)\frac{1}{\eta} \quad . \tag{5}$$

Equation 5 illustrates that $\Delta T \to 0$ in the limit that $P_h \to P_s$. To estimate ΔT, we set $f(T_s,P_s) / f(T_h,P_h) = 1$. This approximation is valid since this ratio departs from unity by less than $5\text{x}10^{-5}$ for the pressure drop considered here.

An upper bound for the uncertainty in η is estimated from Wexler's formulation for $e_w(T)$ [1],

$$\ln e_w = \sum_{j=0}^{2} L_j T^{j-1} + L_3 \ln T \; . \tag{6}$$

Differentiating Eq. 6 with respect to temperature gives,

$$\eta = \frac{d\ln e_w}{dT} = -\frac{L_0}{T^2} + L_2 + \frac{L_3}{T} \; . \tag{7}$$

The uncertainties of L_0, L_2, and L_3 were estimated by assuming that the maximum possible uncertainty for any one of these coefficients would occur if the uncertainties for the other two coefficients were zero. Using this assumption, Eq. 6, and Wexler's stated uncertainty in $e_w(T)$, upper bounds for the respective uncertainties of L_0, L_2, and L_3 were calculated. These uncertainties in L_0, L_2, and L_3 were then combined to yield the uncertainty in η using Eq. 7.

An error propagation analysis of Eq. 5 yields the uncertainty in ΔT in terms of the respective relative uncertainties in η, P_s, and P_h. The uncertainty in T_h is found by adding in quadrature the uncertainties of T_s and ΔT, giving an expanded uncertainty in the frost-point temperature T_h equal to 0.013 °C. Note that the combined expanded uncertainty in T_s of 0.012 °C dominates the uncertainty in T_h.

The LFPG generates sufficiently dry water vapor / gas mixtures that potential sources of additional water vapor and transient adsorption / desorption occurring downstream of the saturator must be minimized. The LFPG employs no expansion valve. A minimum number of electro-polished tubing connections employing metal face seals are used, and no tubing bends are permitted. While transient effects have not been observed, additional studies using atmospheric pressure ionization mass spectrometry (APIMS) are planned.

7. CONCLUSION

For humidity expressed as a mole fraction of water vapor in air, Fig. 2 shows that the expanded (k=2) relative uncertainty produced by the LFPG is < 0.8 %. The major contributions are Type B uncertainties in $e_w(T)$ and $f(T,P)$. We emphasize that the published uncertainties for $e_w(T)$ and $f(T,P)$ are based upon rigorous thermodynamic analyses and measurements of relevant thermodynamic properties [1-3]. These contributions are independent of limitations in the LFPG design. Smaller uncertainties in $e_w(T_s)$ and $f(T_s,P_s)$ also contribute to uncertainty in x and arise from uncertainties in T_s and P_s. These contributions to the uncertainty in x are limited by the LFPG design and measurement system performance.

For humidity expressed in terms of frost-point temperature T_h, the expanded uncertainty of 0.013 °C is dominated by the uncertainty in T_s. Unlike the uncertainty in x, the uncertainty in T_h is essentially independent of uncertainties in $e_w(T)$ and $f(T,P)$ as a result of the small pressure drop inherent in the design of the LFPG. In the limit of zero pressure drop between the saturator and hygrometer, and for fixed mixture composition, the thermodynamic states of the mixtures in the saturator and hygrometer are identical. Consequently $T_h = T_s$ in this limit, a result that is independent of the functional forms used to model $e_w(T)$ and $f(T,P)$.

ACKNOWLEDGEMENTS

We would like to thank the NIST Office of Microelectronics Programs for their support of this work. We also thank Robert Berg and Jack Martinez for carefully reading this manuscript.

REFERENCES

1. Wexler A., *Journal of Research of the National Bureau of Standards*, 1977, **81A**, 5-19
2. Hyland R.W., Wexler A., *Ashrae Transactions*, 1983, **89**
3. Hyland R. W., *Journal of Research of the National Bureau of Standards*, 1975, **79A**, 551-560
4. Scace G. E., Huang P. H., Hodges J. T., Olson D.A., Whetstone, J. R., *Proceedings of NCSL 1997 Workshop and Symposium*, 1997, 657-674
5. *Guide to the Expression of Uncertainty in Measurement*, Geneva, ISO,1993
6. Preston-Thomas H., *Metrologia*, 1990, **27**, 3-10 and 107

Addresses of the Authors:

Gregory E. Scace, NIST, 100 Bureau Dr., Stop 8363, Gaithersburg, MD, USA 20899-8363, E-mail: Gregory.scace@nist.gov, Internet: http://www.nist.gov